The effect of formulations and experimental conditions on in vitro human skin permeation: data from updated EDETOX database

Article (Accepted Version)

The effect of formulations and experimental conditions on in vitro human skin permeation—Data from updated EDETOX database

Eleftherios G. Samaras [a], Jim E. Riviere [b], Taravat Ghafourian [a]*

[a]: Medway School of Pharmacy, Universities of Kent and Greenwich, Central Avenue, Chatham, Kent ME4 4TB, UK; [b]: Center for Chemical Toxicology Research and Pharmacokinetics, 4700 Hillsborough Street, North Carolina State University, Raleigh, USA.

*: Corresponding author, Tel: +441634202952; fax: +441634883927; e-mail: t.ghafourian@kent.ac.uk;

Running head: Modelling Skin Permeation Flux

Abstract

In vitro methods are commonly used in order to estimate the extent of systemic absorption of chemicals through skin. Due to the wide variability of experimental procedures, types of skin and data analytical methods, the resulting permeation measures varies significantly between laboratories and individuals. Inter-laboratory and inter-individual variations with the *in vitro* measures of skin permeation lead to unreliable extrapolations to *in vivo* situations. This investigation aimed at a comprehensive assessment of the available data and development of validated models for *in vitro* skin flux of chemicals under various experimental and vehicle conditions.

Following an exhaustive literature review, the human skin flux data were collated and combined with those from EDETOX database resulting in a dataset of a total of 536 flux reports. Quantitative Structure-Activity Relationship techniques combined with data mining tools were used to develop models incorporating the effects of permeant molecular structure, properties of the vehicle, and the experimental conditions including the membrane thickness, finite/infinite exposure, skin pre-hydration and occlusion.

The work resulted in statistically valid models for estimation of the skin flux from varying experimental conditions, including relevant real-world mixture exposure scenarios. The models indicated that the most prominent factors influencing flux values were the donor concentration, lipophilicity, size and polarity of the penetrant, and the melting and boiling points of the vehicle, with skin occlusion playing significant role in a non-linear way. The models will aid assessment of the utility of dermal absorption data collected under different conditions with broad implications on transdermal delivery research.

Keywords: QSAR, skin, dermal, permeation, absorption, in vitro, decision tree, finite dosing, occlusion, hydration

1. Introduction

Skin is in continuous contact with exogenous molecules. Skin's essential role is to protect the body from absorption of exogenous toxic material such as pesticides that target toxicological endpoints and can have local and systemic effects (Nielsen et al, 2004). Therefore, the European Commission program, REACH, requires extensive risk assessments of all existing chemicals, including exposure via dermal contact (Commission of the European Communities, 2003). Skin is also the focus of research by drug formulators as a site of drug administration, both for local dermatologic conditions as well as for systemic delivery due to the advantages it may offer over other routes of drug delivery (Barry, 2007).

A vast number of studies in the past have compared the *in vitro* and *in vivo* methods for measuring dermal absorption and have come to the conclusion that properly conducted *in vitro* measurements can be used to predict *in vivo* absorption (OECD, 2004a). The OECD Test Guidelines 428 has also confirmed that *in vitro* studies can predict *in vivo* absorption when the correct methodology for both tests is used. *In vitro* methods can vary greatly in terms of the source of skin samples, experimental procedures, and the resulting measurements. These guidelines are flexible in terms of the use of animal or human skin samples (OECD, 2004a, 2004b). In the literature, many of the reported data pertains to the experiments using artificial skin membranes that mimic human skin. In terms of the human skin samples, the skin can be cadaver human skin or surgically removed skin which may be used fresh as viable skin or after certain period of freezing. These are all sources of variability in the reported results. For example, the absorption of benzoic acid and para-aminobenzoic acid were significantly greater in nonviable, compared with viable,

67 metabolically active hairless guinea pig skin (Nathan et al., 1990). Moreover skin samples
68 can be full thickness or dermatomed with varying thicknesses (Wilkinson et al., 2006).

69 Apart from the skin sample, the experimental procedures can also influence the results of the
70 *in vitro* tests. For example, stratum corneum can significantly change its dimensions when
71 exposed for long periods to water (Bouwstra et al., 2003). Experimental approaches vary
72 from studies employing pre-hydrated skin samples, to those using infinite doses which lead to
73 the skin hydration during the period of the experiment, or studies using occlusion of the skin
74 which may lead to some levels of hydration during the experiment, or those employing finite
75 dosing without occlusion which limits the skin hydration. Skin occlusion has been found to
76 enhance the percutaneous absorption of many, but not all topically applied compounds
77 (reviewed by Zhai & Maibach (2001)). On the other hand, unoccluded conditions can
78 simulate the normal exposure situations in everyday life. However, volatile compounds may
79 evaporate under unoccluded conditions and infinite dosing can only take place under
80 occluded conditions (Kligman, 1983; Bronaugh & Stewart, 1985; Baker, 1986). According to
81 OECD (OECD, 2004b), for finite dose experiments, a dose of 1-5 mg/cm^2 or 10 µl/cm^2
82 should be spread on the skin surface and for infinite dose experiments, a dose higher than 10
83 mg/cm^2 or 100 µl/cm^2 is needed in order to obtain steady state conditions from which the flux
84 and k_p can be calculated. In the literature, a full spectrum of application doses can be found
85 with varying duration of exposure and sampling time.

86 The inter- and intra-laboratory variation in *in vitro* percutaneous absorption methodology has
87 been investigated to some extent in the past. In a recent study by van de Sandt et al. (2004)
88 the *in vitro* absorption of several compounds through human and rat skin were determined in
89 different laboratories. In all laboratories the studies were undertaken according to detailed
90 protocols of dose, exposure time, vehicle, receptor fluid, preparation of membranes and
91 analysis. Results of this study showed noticeable differences that may be attributed to the

inter-individual variability in absorption between samples of human skin and differences in skin site and source. Skin thickness only slightly influenced the absorption of benzoic acid and caffeine; however the maximum absorption rate of the most lipophilic compound, testosterone, was clearly higher in laboratories using thin, dermatomed skin membranes.

A vehicle can play a very important role in the penetration of a chemical through the skin. Solubility of a chemical is different in different vehicles hence resulting in different flux and k_p values due to varying levels of saturation (Roberts et al, 2002). A vehicle can promote the penetration of a chemical by having low solubility, in this way a chemical will not be retained in the vehicle (Baker, 1986). In case in the vehicle there are components that can interact with the intercellular lipids of the SC then it is possible that permeation may be enhanced or suppressed (Davis et al., 2002). Formulation ingredients can alter the skin penetration of a compound by affecting the barrier properties of the skin or by changing the partitioning of the compound into the SC. The effect of mixture/formulation components on the skin penetration of a compound depends on the nature of the component, i.e. its chemical structure and physicochemical properties. The relationship between chemical structures of the formulation ingredients and the skin penetration modification can be studied quantitatively using Quantitative Structure–Activity Relationship (QSAR) techniques (Ghafourian et al., 2004; 2010a, 2010b; Riviere and Brooks, 2005, 2011).

As an integral part of the human health risk assessment of chemicals and also to be able to aid drug delivery through skin, it is essential to be able to estimate absorption of chemicals via the dermal route. This is because despite the requirement by REACH for extensive risk assessment of chemicals, it is not practical to measure dermal absorption of the many thousands of industrial chemicals. In reality, estimation of skin absorption is complicated due to the inconsistency of the methods and therefore the inconsistent results of *in vitro*/ *in vivo* tests. The inter-laboratory and inter-individual variations are often high (Van de Sandt et al.,

2004, Chilcott et al., 2005) which may be explained by the huge variety of methods and test systems used for skin permeation experiments. Moreover, methods of calculation and interpretation of results from the complex experimental set-up also varies (Henning et al., 2009). The aim of this study was to investigate the effects of experimental conditions such as membrane thickness, occlusion, hydration, vehicle ingredients and mode of exposure (finite or infinite dosing) on the skin permeation flux. This was achieved through the use of statistical techniques employing a large dataset extracted from EDETOX database and collated from more recent publications. The dataset was large enough to investigate statistically the effects of these variable experimental conditions combined with QSAR linking the skin flux to the chemical structures of the penetrants and the physico-chemical properties of the vehicle mixtures.

2. Methods

2.1. The dataset

The *in vitro* flux of chemicals from human skin measured by flow-through or static cells were obtained from the recent literature (2001-2010) and EDETOX (Evaluations and Predictions of Dermal Absorption of Toxic Chemicals) database (EDETOX, 2010). The compiled data is available as Supplementary Material I. The EDETOX database contains data from *in vitro* and *in vivo* percutaneous penetration studies involving use of different species, cell types and chemicals with a total of 2501 records taken from 341 penetration studies. The EDETOX database gave information about chemical name, vehicle used, origin of the skin sample, membrane thickness, exposure time, length of study, percentage of dose absorbed, percentage recovery, flux, permeation rate (k_p), lag time, where available, and the source publications. Further information with regards to the hydration state, occlusion condition, the volume applied ($\mu l/cm^2$), dose applied ($\mu g/cm^2$) and donor concentration ($\mu g/ml$) was added to the dataset by careful inspection of the original publications.

142 Following an exhaustive literature survey, data from recent publications (2001-2010) was
143 added to the dataset extracted from EDETOX database. The literature survey was performed
144 in the Web of Knowledge with the key worlds; skin absorption, skin penetration, skin
145 permeation, skin permeability, dermal absorption, dermal penetration, dermal permeation and
146 dermal permeability. From resulting 1800 publications all human *in vitro* data were extracted.

147 Data concerning the pre-treated skin samples with a solvent or a penetration enhancer were
148 discarded but pre-treatment with water (hydration) was allowed in the dataset. Absorption
149 measurements from commercial mixtures with unknown constituents or complicated
150 formulations such as liposomes and emulsions were not used. The final working dataset
151 consisted of 536 flux reports containing 272 unique chemicals. The chemicals were either
152 applied as neat (around 10% of the data) or formulated in simple mixtures with the majority
153 of vehicles containing water as a constituent. In a few cases that the formulations were gels,
154 the percentage of constituents were known. In majority of cases the exposure time was 24 h,
155 but it varied from 0.167 to 336 h, and the sampling time between 0.167 and 336 h. The
156 composition of the receptor fluid could vary to allow different additives, pH or solvent types.
157 In many cases, the finite or infinite dosing conditions were explicitly specified in the
158 literature. In other cases, if the application volume was above 100µl it was taken as 'infinite',
159 if donor volume was between 50-100µl then provided that the percentage absorbed was less
160 than 20% it was considered as 'infinite' or otherwise a 'finite' application. An indicator
161 variable was generated to indicate finite or infinite dosing in the statistical analyses with the
162 values of 2 for finite and 1 for infinite dosing. Experimental conditions under which flux was
163 measured were explored further and whether the skin was hydrated prior to the experiment
164 (minimum of 1 hr hydration) and whether the donor compartment was occluded was recorded
165 in the dataset. In order to incorporate these in statistical analysis, states of pre-hydration or

166 occlusion were given a value of '1' where skin was hydrated or occluded and '0' when the
167 skin was not pre-hydrated or occluded.

168 In the dataset the preparation of the skin may vary from full thickness or dermatomed skin, to
169 epidermal membranes. Skin thickness measurements were specified in many publications in
170 mm. If only a description was provided in the literature, the full thickness skin was taken as 2
171 mm, epidermis as 0.8 mm and SC as 0.2 mm thick.

172 **2.2. Molecular descriptors of permeants:**

173 Simplified Molecular Input Line Entry Specifications (SMILES) of penetrants were obtained
174 online from ChemSpider (2010), PubChem (2010), and Sigma-Aldrich (2010). If the
175 compound structure was not available in these databases, reference books or ChemBioFinder
176 (2010) were used to find the molecular structure, then the structure was drawn in
177 ACD/ChemSketch software (Advanced Chemistry Development, Inc., Canada) and SMILES
178 codes were obtained. The molecular descriptors (375) were calculated using ACD labs/LogD
179 Suite version 12.01 (Advanced Chemistry Development, Inc., Canada) and Molecular
180 Operating Environment (MOE) version 2011.10 (Chemical Computing Group Inc., Canada).
181 The molecular descriptors included physical properties (e.g. partition coefficient and
182 molecular weight), subdivided surface areas, atom and bond counts, molecular connectivity
183 and kappa shape indexes, adjacency and distance matrix descriptors, partial charge
184 descriptors, potential energy descriptors, MOPAC descriptors, and conformation dependent
185 charge descriptors.

186 **2.3. Properties of the mixture (vehicle):**

187 The physico-chemical properties of mixture components such as boiling point, melting point,
188 density, log P, and solubility were obtained through SRC PhysProp database (2010), Sigma
189 Aldrich website (2010), and ChemSpider (2010). For pharmaceutical excipients such as

polyethyleneglycols (PEGs), petrolatum and mineral oil the properties were obtained from Rowe et al (2009). Average of the physicochemical properties for every solvent mixture was calculated for the liquid ingredients, e.g. boiling point of the vehicle. The effect of solid solutes (including the permeants) on boiling and melting points were calculated using the principles of the colligative properties (Sinko et al 2011). Therefore, boiling point elevation (ΔT_b) and freezing point depression (ΔT_f) due to the dissolved material can be calculated by equations (1) and (2) respectively.

$$\Delta T_b = \text{molality} * K_b * i \qquad (1)$$

$$\Delta T_f = \text{molality} * K_f * i \qquad (2)$$

In equation (1) and (2), K_b and K_f are ebullioscopic and cryoscopic constants specific for the solvent and *i* is Van't Hoff factor. The ebullioscopic (K_b) and cryoscopic constant (K_f) were obtained from the literature (Moore, 1972) and were averaged for the solvent mixtures.

2.4. Development and Validation of models:

Logarithm of steady state flux showed normal distribution and therefore this was used for statistical analysis and development of the mathematical models. Before model development, the data were assessed using a simple semi-mechanistic model involving a linear relationship between log Flux and simple parameters such as donor concentration (as in Fick's law of diffusion), partition coefficient and molecular size (as in Potts and Guy's model (1992)) and an index of molecular polarity. After establishing a preliminary linear relationship, the outliers were identified and, where appropriate, the identified outliers were removed from the dataset.

The dataset was sorted according to log Flux values and partitioned into training and test sets by taking every fourth compound as the test set compound, achieving the ratio of three to one for training and test sets. Two main methods were used for the development of QSAR models

and investigating the effect of experimental variables. These were stepwise regression analysis using MINITAB statistical software ver 15.1.0.0 and non-linear method of RT (Regression Trees) in STATISTICA Data Miner software 9.1. These methods can be considered as variable selection tools for the development of linear (stepwise regression) and non-linear (RT) models with best fit to the training set data. Each of these methods can also allow the user to manipulate the statistically selected variables. Therefore, interactive RT data-mining tool was utilised to evaluate the variables of experimental conditions for each split. In RT method, several stopping criteria were examined. These included either, the minimum number of 11, 22 and 40 compounds, or the minimum fraction of 0.05, 0.02 and 0.01 to the total number of compounds for partitioning. The default values were used for the maximum number of levels set at 10 and the maximum number of nodes at 1000. For the V-fold cross-validation, seed for random number generator was set to 1 and the v value to 10.

In order to compare the validity of the RT and regression models, models were generated using training set compounds and the prediction accuracy was assessed by comparing the average error levels of the estimation of log flux for the test set compounds. The error criterion was Mean Absolute Error (MAE) calculated for the test set.

3. Results

For the development of predictive models and investigation of the effects of various experimental, vehicle or permeant variables, the collated dataset was first refined and the outliers were removed. The investigation was then focused on the development of a series of models with specific emphasis on the descriptors of *in vitro* experimental conditions and vehicle properties. Finally the models were validated and compared in terms of the accuracy of the skin flux predictions.

3.1 The dataset

238 The collated dataset comprised work reported in a wide range of literature where the skin
239 permeation measurements could pursue a large variety of goals ranging from *in vivo* / *in vitro*
240 correlation studies (Dick et al., 1995) to pharmaceutical formulation optimisation (Dias et al.,
241 1999) which could include chemical enhancers (Patil et al., 1996). Furthermore, a large
242 volume of the literature concerns the study of the effect of experimental conditions such as
243 the skin type and area of the skin (Wilkinson & Williams, 2002), pH (Sznitowska et al.,
244 2001), mixture components (Santos et al., 2010), and receptor phase composition (Surber et
245 al., 1991) on the *in vitro* absorption of compounds. Therefore large inter-laboratory and inter-
246 individual variations are very common. In the current exercise, a dataset with best internal
247 consistency is required in order to investigate the effects of some of the variable experimental
248 conditions as well as the vehicle and the permeant chemical structures. Therefore, the dataset
249 was initially assessed through the use of a simple semi-mechanistic model and the extreme
250 outliers were identified. In accordance with the Fick's Law of diffusion and the well-accepted
251 model of Potts and Guy (1992), this initial model for flux was formulated to comprise donor
252 concentration (according to Fick's Law of diffusion), a size descriptor and lipophilicity index
253 (log P). In addition a polarity descriptor was also incorporated in the model as informed by
254 previous studies (Tayar et al., 1991; Liou et al 2009). Multiple regression analysis was used
255 to fit the data and only the statistically significant parameters with P values below 0.05 were
256 allowed in the model (equation (3)).

257 $$\log \text{Flux} = 1.63 + 0.000002\,[\text{Donor}] - 2.83\,\text{PSA/SA} - 0.00417\,\text{MV} \qquad (3)$$

258 $S = 1.25,\ r^2 = 0.376,\ N = 499,\ F = 99.5$

259 In equation (3), [Donor] is the donor concentration, PSA/SA is the polarity index represented
260 by the ratio of polar surface area to the total surface area, and MV is the size descriptor,
261 molar volume. It must be noted that despite the fact that lipophilicity of permeants is believed
262 to be a major factor in skin permeation of compounds, in this case octanol/water partition

263 coefficient (log P) was not statistically significant and therefore not included in equation (3).
264 Figure 1 shows the plot between observed and calculated log Flux by equation (3), with the
265 regression line between these two showing an intercept of 0.000 and a coefficient of 1.00.

266 Chemicals with standardised residuals greater than 1.5 and less than -1.5 were marked as
267 outliers; these are highlighted in Figure 1(a). A list of these outliers and some explanations
268 for their deviations has been provided in the Supplementary material I. Most notably, out of
269 22 compounds, 9 are steroids with the flux values taken from Scheuplein et al (1969). These
270 skin permeability measurements have been reported to be consistently lower than those
271 measured by several other groups (Johnson et al 1995). The outliers were removed from
272 subsequent analyses.

273

274 **3.2 The models developed by statistical variable selection**

275 Molecular descriptors of the penetrants, properties of the vehicles and indicator variables for
276 experimental conditions of flux measurement, namely finite/infinite dosing, skin pre-
277 hydration, occlusion and also the skin thickness in mm were used in stepwise regression
278 analysis and Regression Trees analysis. Donor concentration was the first (and the most
279 significant) variable controlling the flux of various compounds as indicated by both statistical
280 methods. Equation (4) is the linear regression model developed by stepwise regression
281 analysis. Figure 2 shows RT model (1). A description of the parameters used in all models
282 has been provided in the notation section.

283 log Flux = - 1.92 + 0.000001 [Donor] - 0.00570 MW + 0.00235 BP-MP(mix) + 3.96 vsurf_G
284 + 0.0137 SlogP_VSA4 - 1.93 fiAB - 0.343 VAdjMa (4)

285 *S = 0.948, r^2 = 0.558, N = 454, F = 80.41*

The parameters of equation (4) consists of donor concentration, a vehicle property representing the difference between boiling and melting points of the vehicle mixture (BP-MP(mix)), and five other parameters representing molecular descriptors of the permeants. The model generated by RT consists of donor concentration and three molecular descriptors for the penetrants (Figure 2). Table 1 gives the statistical parameters of the RT model.

3.3 Models incorporating the membrane thickness

Skin thickness is thought to play a significant role in dermal absorption of chemicals. Permeation through viable full thickness skin membranes has been shown to be less than permeation through only the epidermis (Cnubben et al. 2002). The membrane thickness in the dataset varied between 0.2 for SC and 2 mm for the full thickness human skin. Membrane thickness (in mm) was incorporated in linear regression (equation (5)) and RT model (Figure 3).

logFlux = - 1.67 + 0.000001 [Donor] - 0.00561 MW + 0.0140 SlogP_VSA4 - 1.95 fiAB + 0.00192 BP-MP(mix) + 3.82 vsurf_G - 0.312 VAdjMa - 0.201 Thickness (5)

S = 0.943 r^2 = 0.564 N = 454 F = 71.9 P < 0.001

Although r^2 of equation (5) shows only a slight improvement to equation (4), the thickness parameter is statistically significant in this equation (P = 0.014). Wilkinson et al. (2004, 2006) studied the influence of skin thickness on percutaneous penetration using caffeine, testosterone, butoxyethanol and propoxur. They concluded that a complex relationship exists between skin thickness, lipophilicity of the penetrant, and percutaneous penetration and distribution. Therefore, due to the uneven effect of skin thickness on the penetration of different chemicals of varied lipophilicity (or other physicochemical properties), a linear relationship such as equation (5) cannot adequately represent the effect of thickness.

310 Accordingly, incorporation of skin thickness in the RT analysis could be more beneficial. In
311 RT model (2) (Figure 3), this parameter was used in the first split and the tree was allowed to
312 select other parameters of the highest statistical significance. The RT model involved skin
313 thickness, donor concentration and four molecular descriptors of the penetrants.

314

315 **3.4 Models incorporating the finite or infinite dosing**

316 The dataset included in this work contained steady state and maximum flux obtained under
317 finite and infinite dose exposures. In infinite dose, the concentration of the solution applied to
318 the skin does not significantly change over time. Therefore a maximum flux can be achieved
319 and maintained during the course of the experiment (steady state flux). However in finite
320 dose exposures the amount of test preparation applied to the skin will reduce over time and
321 therefore the maximum flux cannot be maintained. In order to incorporate the dose exposure
322 condition, an indicator variable taking a value of 2 for finite and 1 for infinite condition was
323 used. Out of 513 flux values with known exposure conditions, 143 and 370 were obtained
324 under finite and infinite exposure conditions, respectively. The graph between observed log
325 flux values and the log flux calculated by equation (4) indicates differing lines of best fit to
326 the data obtained under infinite or finite dose exposures (Figure 1(b)). These regression lines
327 were compared using general linear model (GLM). The results, reported in Table 2, indicate
328 statistically different slopes and intercepts for finite and infinite exposures. Moreover, when
329 included in the regression analysis, the indicator variable for finite/ infinite dose was
330 statistically significant with a P value of 0.000 (equation (6)).

331 Log Flux = - 1.08 + 0.000001 [Donor] - 0.00592 Weight + 0.00992 SlogP_VSA4 - 1.85 fiAB
332 + 0.00230 BP-MP(mix) + 3.55 vsurf_G - 0.293 VadjMa - 0.391 Infinite/Finite (6)

333 $S = 0.936$ $r^2 = 0.572$ $N = 453$ $F = 74.1$ $P < 0.001$

334 The negative coefficient of Infinite/Finite (indicator variable) indicates higher flux values
335 when measured under infinite dose exposures.

336 RT analysis with the inclusion of this indicator variable as the first partitioning parameter was
337 performed using Interactive Trees application in STATISTICA. The RT model (RT (3))
338 indicated somewhat higher average flux for infinite exposure experiments (Figure 4).

339

340 **3.5 Models incorporating the skin pre-hydration**

341 The stratum corneum normally contains 5-20% water, but it can contain upto 50% water
342 when hydrated. Hydration can affect the permeability of the skin to chemicals (Roberts &
343 Walker, 1993). Pre-hydration of the skin before the start of the experiment is very common in
344 infinite dose procedures in order to maintain the consistency of the membrane during the
345 course of the experiment. In this dataset, 187 data points used pre-hydrated skin and 317 data
346 points employed dry skin. Figure 1(c) identifies the lines of best fit to the data obtained with
347 pre-hydrated or dry skin. Comparing these lines by GLM (Table 2) shows that pre-hydration
348 of the skin does not affect the slope of the line, although the intercepts are statistically
349 different. When used in combination with descriptors of equation (4), the indicator variable
350 for skin pre-hydration is not statistically significant at $P<0.05$. However, with a P value of
351 0.077, pre-hydration of skin has a positive effect on skin flux.

352 One reason for the insignificant effect of pre-hydration could be attributed to the fact that at
353 least with infinite dose experiments, stratum corneum can quickly hydrate during the course
354 of the experiment. Moreover, even in finite dose experiments, many studies are conducted
355 under occluded conditions, which may lead to some levels of hydration. On the other hand,
356 the extent of the hydration-related permeability change for different chemicals is not well

elucidated. For example, it has been shown that the increase of hydration due to occluded conditions does not always guarantee an increase in penetration rates (Bucks et al. 1991).

In conclusion, as with membrane thickness, hydration of skin may have different levels of effects on the flux of compounds with varying physicochemical properties. Therefore, the effect is expected to be captured better in the non-linear models such as RT. The indicator variable for skin pre-hydration was incorporated as the first partitioning parameter in interactive RT analysis. The model (RT(4)) indicated higher average flux from pre-hydrated skin than from dry skin with the average log flux difference of 0.144 (Figure 5).

3.6 Models incorporating the occlusion state of the skin

Occlusion of the skin can lead to the gradual hydration of the skin during the course of the *in vitro* tests even during finite exposures where only a small volume of dose is applied. Therefore, as with hydration, flux values of various compounds is expected to be affected by occlusion of the skin. Out of 481 flux values with reported occlusion condition, 287 and 194 were performed under occluded and non-occluded conditions respectively. Indicator variable for occlusion was not statistically significant when incorporated in the regression analysis (P=0.506). The graph between observed and calculated log Flux using equation (4) gives similar slopes but differing intercepts for the data obtained under occluded or non-occluded conditions (Figure not shown, see GLM results in Table 2). To explore the effect of occlusion further, it was incorporated in RT analysis. The resulting RT model (Figure 6, RT (5)) indicates that the average flux obtained under occluded conditions is higher than the average flux measured under non-occluded conditions by 0.66 log units.

3.7. Models incorporating the vehicle effects

Stepwise regression analysis selected the difference between boiling and melting points of the vehicle mixtures to represent the effect of vehicle on the flux (equation (4)). However, a vehicle descriptor is missing from most RT models with the exception of RT (4) which includes a vehicle descriptor (boiling point of vehicles). The effect of vehicle properties on the flux was further analysed by incorporating boiling point, melting point and the gap between these in the interactive RT. The model obtained using BP-MP(mix) (Presented as RT model (6) in Figure 7) had the lowest standard error. According to this model, flux is higher if the donor mixture has a larger gap between the melting and boiling points of the vehicle. Table 1 shows that RT (6) has the lowest mean absolute error amongst all RT models. This may indicate the high significance of the vehicle properties in the skin absorption.

3.8. Validity and Reliability of the models

In any QSAR modelling, it is essential to examine the validity of the models for future predictions. This is also important due to the large number of molecular descriptors that are initially considered for the descriptor selection, which may result in chance correlations and poor generalisation (Konovalov et al., 2008). In this work, every effort have been made to assess the models by considering the interpretability of the models and agreement with the previous knowledge. Moreover, regression models (equations (4) – (6)) and RT models (1) – (6) were validated by using the regression equations and RT models developed for the training set for the estimation of the flux values of the test set. Table 3 gives the mean absolute error of log Flux estimation for the test set compounds and the number of test set compounds for which the models are able to provide the estimation. The lowest average error is achieved with RT model (5) followed by RT (4) and then regression equation (6) and RT (3).

4. Discussion

Inter-laboratory and inter-individual variations are very common in the *in vitro* measures of skin permeation. This has been attributed to a number of experimental variables including differences in skin samples' thickness, skin hydration, occlusion of the skin, infinite or finite dosing and vehicle ingredients. The dataset gathered here provided an excellent resource for development of QSAR models which also incorporate the effect of various experimental variables. The models can elucidate the effects of various parameters on the *in vitro* measures of skin permeation. The statistical analysis involved linear stepwise regression and non-linear regression tree analyses. Regression tree analysis has the advantage that it does not assume linearity in the relationship between the flux and any of the variables. The statistically selected parameters by these methods were donor concentration, several molecular descriptors of the permeants and, in case of stepwise regression, the difference between boiling and melting points of the donor mixtures (See equation (4) and Figure 2).

The relevance of the donor concentration of the permeant to the flux is clear as the higher the concentration the higher the driving force and the flux according to Fick's law of diffusion, and this can be observed in both the linear regression and RT models. In equation (4), the difference between the boiling and the melting points of the donor mixture shows a positive effect on the flux. Ghafourian et al (2010a) had observed a similar effect previously for a different dataset that involved various combinations of five different vehicle ingredients and 16 permeants. The reason for this effect can be attributed to the better penetration of low melting point vehicles carrying the drug along into and out of the skin (Monene et al., 2005). For example, the formation of eutectic mixtures between drug and some vehicles has been proposed as the reason for skin penetration enhancement by some terpenes (Stott et al.,

1997). On the other hand, the magnitude of the gap between melting and boiling points indicates certain characteristics in the molecular structure as it is believed that more symmetrical molecules have higher melting points and lower boiling points (Slovokhotov et al., 2007). Presence of molecular weight of the permeants in equation (4) is in agreement with the model proposed by Potts and Guy (1992). The molecular descriptor vsurf_G represents the molecular globularity (Cruciani et al., 2000), and with a positive coefficient, indicates higher flux values of non-spherical molecules that may be elongated or planar shaped. SlogP_VSA4 is a lipophilicity descriptor for the permeants which is known to play a major role in skin permeation (Bouwman et al., 2008). FiAB is the fraction of ionization of molecules at pH 7.4. In the lipophilic environment of the stratum corneum ionized molecules are expected to permeate more slowly than unionized molecules (Watkinson et al., 2009). The last molecular descriptor of the permeant in equation (4) (VadjMa) represents the number of strong bonds (ionic, covalent, polar covalent). The number of strong bonds is related to the size of the molecule therefore the larger molecules are expected to have low permeation rates.

Similarly, according to RT (1), the requirements of a high skin flux are high donor concentration, small positively charged molecular surface area (PEOE_VSA_POS), large surface area of non-acidic hydrogen bond acceptors such as ether and ketone groups (vsa_acc), with a complex effect of hydrophobic volume (vsurf-D6) probably indicating the negative effect of molecular size at nodes ID 4, 5, 14 and 15, and the positive effect of hydrophobicity at nodes ID 6, 7, 10 and 11.

As one of the objectives of the investigation was to incorporate the effects of the *in vitro* experimental conditions in the models, further RT and linear regression models were developed with the incorporation of parameters such as skin thickness, dosing conditions and

453 states of pre-hydration or occlusion of the skin. This led to RT models (2) – (6) and equations
454 (5) – (6), the statistical performance and the validity of which can be compared.

455 Within the linear regression equations, the order of significance of the experimental variables,
456 as deduced from the P-values, were BP-MP(mix) in equation (4), indicator variable for finite
457 or infinite dosing in equation (6) (P=0.000), skin thickness in equation (5) (P=0.014), and
458 pre-hydration (P=0.077), with occlusion of the skin not being significant (P>0.10). Validation
459 of the models also revealed a lower average error (for test set) for the model incorporating
460 mode of exposure as opposed to the skin thickness (Table 3).

461 According to the mean absolute error of the calculated values (reported in Table 1), the order
462 of significance of the non-linear RT models is models incorporating: BP-MP(mix), occlusion,
463 pre-hydration, and mode of exposure. However, validation of these models indicated the
464 highest validity of the model incorporating occlusion state of the skin (RT (5)) followed by
465 the model incorporating both skin pre-hydration and boiling point of the donor phase (RT (4))
466 and then the model incorporating the mode of exposure (RT (3)) (see Table 3). This
467 conclusion, in association with the fact that experimental parameters of occlusion and pre-
468 hydration perform better in non-linear models, indicate that occlusion and skin pre-hydration
469 have important but complex and non-linear effects on the skin absorption.

470 It has previously been observed that occlusion and skin hydration may affect the skin
471 permeation of different permeants differently (Bucks et al. 1991). For example, comparing
472 the skin permeability measure obtained from Fickian diffusion model and that obtained from
473 the transient skin permeation profiles, Tang et al Tang et al (2002) reported significantly
474 increased skin permeability due to hydration for highly hydrophilic compounds while skin
475 permeation of lipophilic compounds were comparable between the hydrated and non-
476 hydrated states of skin. Similar nonlinear effects have also been reported for the effect of skin
477 thickness on permeation of drugs with various lipophilicities (Wilkinson et al., 2004). The

effect of occlusion may be explained by gradual skin hydration, or evaporation of the volatile penetrants and/or the vehicles. In the study of Sartorelli et al. (2000) a 5 to 10 fold increase in permeability of the stratum corneum was noted when the skin was occluded. In the study of Jung et al. (2003) where catechol was applied in ethanol, occluded conditions resulted in 78% of the applied dose permeating compared with 55% in non-occluded samples.

Figures 2-7 show the RT models incorporating skin thickness (RT (2)), mode of exposure (RT (3)), pre-hydration (RT (4)), occlusion (RT (5)), and vehicle boiling and melting point gaps (RT (6)). RT model (2) indicated that the average log Flux with skin thickness of ≤1.21 mm is much higher than with skin samples of >1.21 mm thick (average log flux of 1.124 and 0.252 respectively). The model also indicates higher *in vitro* skin flux with large donor concentrations, low polarity index (indicated by high GCUT_PEOE_1), small positively charged molecular surface area (PEOE_VSA_POL), small hydrophilic volume (vsurf_W1) and small molecular size (chi1v_C).

RT (3) indicates that compounds will have higher *in vitro* flux values when applied in infinite doses, with high donor concentrations, and if they have high lipophilicity (GCUT_SLOGP_1), small molecular size (chi0 and GCUT_SMR_3) with high polarisability (SMR_VSA6) or hydrophilic surface (vsurf_CW3). According to RT (4), compounds with small molecular size (KierA1), applied in higher concentrations, especially those with small hydrophobic surface area (vsa_hyd), will be absorbed very well from pre-hydrated skin samples. Similarly, from (initially) dry skin samples, compounds with small molecular size (chi0v) applied in high concentrations are absorbed with the highest flux, while those applied in lower concentrations, with a small molecular size (wienerPath), having a high polarisability (GCUT_SMR_0), if administered in a low boiling point vehicle are absorbed the least. RT (5) indicates a higher flux from occluded skin samples for chemicals applied in high concentrations having a small molecular size (chiv_C), while those applied in low doses

503 are expected to have low flux values especially if the molecules have high hydrogen bonding
504 donor capacity (vsurf_HB5). From non-occluded skin samples, compounds with relatively
505 high solubility (logS) applied in high doses also show high flux values, while those with low
506 solubility, large sum of positive atomic charges (leading to low relative positive charge,
507 PEOE_RPC+) or low polar volume (vsurf_Wp2) show the least flux values. RT (6) shows
508 that flux is higher if the donor mixture has a higher gap between melting and boiling points
509 and the molecular size of the permeant is small (large chiv_C), especially if applied in higher
510 concentrations. If BP-MP(mix) is small, then molecules with small molecular size (KierA1)
511 still have higher flux values than the large molecular size compounds specially if applied in
512 higher concentrations.

513 It can be noted that skin thickness or the indicator variables for the experimental conditions,
514 namely pre-hydration, finite/ infinite dosing or occlusion, are not selected by stepwise
515 regression analysis (equation (4)) or regression tree (RT (1). Given the higher prediction
516 accuracy of some of the models that incorporate experimental conditions, this may be
517 attributed to the incorporation of extremely high number of permeant molecular descriptors in
518 stepwise regression and RT analyses (a total of 375 descriptors) in comparison with the few
519 variables of experimental conditions, leading to inadequate variable selection by these
520 statistical methods.

521 In conclusion, comparing all linear and nonlinear models (Table 3), it can be seen that the
522 generally, RT models perform better in terms of the prediction accuracy for the test set. The
523 lowest average error is achieved with RT model (5) followed by the RT (4) and then
524 regression equation (6) and RT (3). The most valid model, RT (5) involves the occlusion
525 indicator variable, donor concentration, and five permeant descriptors implying the negative
526 effects of molecular size and hydrogen bonding donor ability on flux from occluded skin, and
527 positive effect of aqueous solubility, and polar volume and negative effect of relative positive

charge when the skin is not occluded. It must be noted that the number of test compounds for which estimation has been made possible is different, depending on the availability of the model parameters.

In both regression and RT models donor concentration of the permeant is the most important parameter related to the skin flux. This is expected since concentration is the driving force for passive diffusion of molecules across the skin. A variety of permeant parameters have been employed in the models, with majority implying the negative impacts of the large molecular size and hydrophilicity, while a certain level of lipophilicity and polarisability has been indicated as a positive effect on the flux.

The statistical analyses and models reported in this work provide a suitable method for homogenizing the *in vitro* flux values measured under varying experimental and exposure conditions and will provide reasonable estimates of the flux values under other experimental conditions. It is expected that the results will benefit *in vivo* estimations using the *in vitro* flux estimates.

Notation

Model parameters	**Description**
[donor]	donor concentration (μg/ml)
BP-MP(mix)	difference between the boiling and melting points of the mixture (donor phase)
chi0	Zero order molecular connectivity index [a]
chi0v	Zero order valence molecular connectivity index [a]
chi1v_C	First order carbon valence connectivity index [a]
fiAB	fraction of molecules ionized as anion and cation at pH 7.4
GCUT_PEOE_1	The GCUT descriptors are calculated from the eigenvalues of a modified graph distance adjacency matrix. Each *ij* entry of the adjacency matrix takes the value $1/\mathrm{sqr}(d_{ij})$ where d_{ij} is the (modified) graph distance between atoms *i* and *j*. The diagonal takes the value of the PEOE partial charges. The resulting eigenvalues are sorted and the

	smallest, 1/3-ile, 2/3-ile and the largest eigenvalues are reported [b]
GCUT_SLOGP_1	The GCUT descriptors using atomic contribution to logP instead of partial charge [b]
GCUT_SMR_0	The GCUT descriptors using atomic contribution to molar refractivity using the instead of partial charge [b]
GCUT_SMR_3	The GCUT descriptors using atomic contribution to molar refractivity instead of partial charge [b]
Infinite/Finite	Indicator variable indicating infinite or finite exposures taking a value of 2 for finite and 1 for infinite dosing
KierA1	First alpha modified shape index, also correlated with molecular size [a]
KierA3	Third alpha modified shape index, informing centrality of branching with large values representing location of branching at the extremities of the molecule [a]
Logs	Log of the aqueous solubility (mol/L) calculated by MOE from an atom contribution linear atom type model [b]
MW	molecular weight
Occlusion	Indicator variable for occlusion of the skin during *in vitro* test
PEOE_RPC+	Relative positive partial charge: the largest positive atomic partial charge divided by the sum of the positive partial charges [b]
PEOE_VSA_POS	Total positive van der Waals surface area. This is the sum of the van der Waals surface area of atoms with non-negative partial charges [b].
Pre-hydration	Indicator variable for pre-hydration of the skin prior to the *in vitro* test
SlogP_VSA4	sum of van der Waals surface area of atoms with log P contributions in the range of (0.1-0.15) [b]
SMR_VSA6	Sum of the van der Waals surface area of atoms with atomic contribution to molar refractivity in the range (0.485, 0.56) [b].
Thickness	Skin thickness
VAdjMa	vertex adjacency information which depends on the number of heavy-heavy bonds [b]
vsa_acc	Approximation to the sum of VDW surface areas of pure hydrogen bond acceptors (not counting acidic atoms and atoms that are both hydrogen bond donors and acceptors such as -OH) [b].
vsa_hyd	Approximation to the sum of VDW surface areas of hydrophobic atoms [b]
vsurf_CW3	Capacity factor representing the ratio of the hydrophilic surface over the total molecular surface. These are calculated at eight different energy levels [c]
vsurf_D6	Volume that can generate hydrophobic interactions. VolSurf computes hydrophobic descriptors at eight different energy levels [c]
Vsurf_EWmin1	The lowest hydrophilic interaction energy
vsurf_G	The molecular globularity – how spherical a molecule is, where values above 1 is non-perfect spheres [c]
vsurf_HB5	H-bond donor capacity, representing the molecular envelope which can generate attractive H-donor interactions with carbonyl oxygen probe. The descriptors are computed at six different energy levels [c].
vsurf_W1	Hydrophilic volume describing the molecular envelope which attractively interacts with water molecules at eight different energy levels [c].
vsurf_Wp2	Polar volume [c]
wienerPath	Wiener path number: half sum of all the distance matrix entries [b]

545 [a]: Hall and Kier (1991); [b]: MOE (2011); [c]: Cruciani et al. (2000)

546

547 **Abbreviations Used**

548 GLM, General Linear Model; MAE, Mean Absolute Error; QSAR, Quantitative Structure–
549 Activity Relationship; RT, Regression Trees; SC, Stratum Corneum; SMILES, Simplified
550 Molecular Input Line Specifications

551

552 **Acknowledgement**

553 Eleftherios Samaras was supported by Medway School of Pharmacy.

554 **Supplementary Material Available**

555 Supplementary material I is the data used for the modelling. List of these outliers and some
556 explanations for their deviations have been provided in the supplementary material II.

557 **References**

558 Baker, H., 1986. The skin as a barrier, in: Rock, A. (Eds.), Textbook of dermatology. Blackwell
559 Scientific, Oxford, pp. 355-365.

560 Barry, B.W., 2007. Transdermal drug delivery, in: Aulton, M.E. (Eds.), Aulton's Pharmaceutics,
561 the Design and Manufacture of Medicines (Third Edition). Churchill Livingstone Elsevier, pp.
562 580-585.

563 Bouwman, T., Cronin, M.T.D., Bessems, J.G.M., van de Sandt, J.J.M., 2008. Improving the
564 applicability of (Q)SARs for percutaneous penetration in regulatory risk assessment. Human Exp.
565 Toxicol. 27, 269-276.

566 Bouwstra, J.A., de Graaff, A., Gooris, G.S., Nijsse, J., Wiechers, J.W., van Aelst, A.C., 2003.
567 Water distribution and related morphology in human stratum corneum at different hydration
568 levels. J. Invest. Dermatol. 120, 750-758.

569 Bronaugh, R.L., Stewart, R.F., 1985. Methods for *in vitro* percutaneous absorption studies IV: the
570 flow-through diffusion cell. J. Pharm. Sci. 74, 64-67.

571 Bucks, D., Guy, R., Maibach, H., 1991. Effects of occlusion, in: Bronaugh, R.L., Maibach, H.I.
572 (Eds.), *In Vitro* Percutaneous Absorption: Principles, Fundamentals and Applications. CRC Press,
573 Boca Raton FL, pp. 85-114.

574 ChemBioFinder. CambridgeSoft. accessed Nov 2010 – Feb 2011. Available from:
575 http://www.cambridgesoft.com/databases.

ChemSpider Home Page. accessed September 2010. Available from: http://www.chemspider.com/.

Chilcott, R.P., Barai, N., Beezer, A.E., Brain, S.I., Brown, M.B., Bunge, A.L., Burgess, S.E., Cross, S., Dalton, C.H., Dias, M., Farinha, A., Finnin, B.C., Gallagher, S.J., Green, D.M., Gunt, H., Gwyther, R.L., Heard, C.M., Jarvis, C.A., Kamiyama, F., Kasting, G.B., Ley, E.E., Lim, S.T., McNaughton, G.S., Morris, M.H., Nazemi, M.A., Pellett, J., du Plessis, Y.S., Quan, S.L., Raghavan, M., Roberts, W., Romonchuk, A., Roper, C.S., Schenk, D., Simonsen, L., Simpson, A., Traversa, B.D., Trottet, L., Watkinson, A., Wilkinson, S.C., Williams, F.M., Yamamoto, A., Hadgraft, J., 2005. Inter- and intra-laboratory variation of *in vitro* diffusion cell measurements: An international multi-centre study using quasi-standardised methods and materials. J. Pharm. Sci. 94, 632-638.

Cnubben, N.H., Elliot, G.R., Hakkert, B.C., Meuling, W.J., van de Sandt, J.J., 2002. Comparative *in vitro – in vivo* percutaneous penetration of the fungicide *ortho*-phenylphenol. Regul. Toxicol. Pharmacol. 35, 198-208.

Commission of the European Communities. Proposal for a Regulation of the European Parliament and of the Council Concerning the Registration, Evaluation, Authorisation and Restriction of Chemicals (REACH), establishing a European Chemicals Agency and amending Directive 1999/45/EC and Regulation (EC) {on Persistent Organic Pollutants}.; 2003. Available from: http://europaeuint/comm/enterprise/chemicals/chempol/whitepaper/reachhtm.

Cruciani, G., Crivori, P., Carrupt, P.A., Testa, B., 2000. Molecular fields in quantitative structure permeation relationships: the VolSurf approach. J. Mol. Struct. – THEOCHEM. 503, 17-30.

Davis, A.F., Gyurik, R.J., Hadgraft, J., Pellett, M.A., Walters, K.A., 2002. Formulation strategies for modulating skin permeation, in: Walters, K.A. (Eds.), Dermatological and transdermal formulations (Drugs and the Pharmaceutical Sciences Vol 119). Marcel Dekker, New York, pp. 271-317.

Dias, M., Farinha, A., Faustino, E., Hadgraft, J., Pais, J., Toscano, C., 1999. Topical delivery of caffeine from some commercial formulations. Int. J. Pharm. 182, 41–47.

Dick, D., Ng, K.M.E., Sauder, G.N., Chu, I., 1995. *In vitro* and *in vivo* percutaneous absorption of 14C-chloroform in humans. Hum. Exp. Toxicol. 14, 260-265.

EDETOX Database. created by the University of Newcastle. accessed June 2010. Available from http://edetox.ncl.ac.uk/

El Tayar, N., Tsai, R.S., Testa, B., Carrupt, P.A., Hansch, C., Leo, A., 1991. Percutaneous penetration of drugs – A quantitative structure permeability relationship study. J. Pharm. Sci. 80, 744-749.

Ghafourian, T., Samaras, E.G., Brooks, J.D., Riviere, J.E., 2010a. Modelling the effect of mixture components on permeation through skin. Int. J. Pharm. 398, 28-32.

Ghafourian, T., Samaras, E.G., Brooks, J.D., Riviere, J.E., 2010b. Validated models for predicting skin penetration from different vehicles. Eur. J. Pharm. Sci. 41, 612-616.

Ghafourian, T., Zandasrar, P., Hamishekar, H., Nokhodchi, A., 2004. The effect of penetration enhancers on drug delivery through skin: a QSAR study. J. Controlled Release. 99, 113–125.

Hall, L.H., Kier, L.B., 1991. The Molecular Connectivity Chi Indices and Kappa Shape Indices in Structure-Property Modeling, in: Boyd, D., Lipkowitz, K. (Eds.), Reviews in computational chemistry. VCH, New York, pp. 384–385.

Henning, A., Schaefer, U.F., Neumann, D., 2009. Potential pitfalls in skin permeation experiments: Influence of experimental factors and subsequent data evaluation. Eur. J. Pharm. Biopharm. 72, 324-331.

622 Johnson, M.E., Blankschtein, D., 1995. Langer, R., Permeation of steroids through human skin. J.
623 Pharm. Sci. 84, 1144-1146.

624 Jung, C.T., Wickett, R.R., Desai, P.B., Bronaugh, R.L., 2003. *In vitro* and *in vivo* percutaneous
625 absorption of catechol. Food Chem. Toxicol. 41, 885-895.

626 Kligman, A.M., A biological brief on percutaneous absorption. 1983. Drug Dev. Ind. Pharm. 9,
627 521-560.

628 Konovalov, D.A., Llewellyn, L.E., Vander Heyden, Y., Coomans, D., 2008. Robust cross-
629 validation of linear regression QSAR models. J. Chem. Inf. Model. 48, 2081-2094.

630 Liou, Y.B., Ho, H.O., Yang, C.J., Lin, Y.K., Sheu, M.T., 2009. Construction of a quantitative
631 structure-permeability relationship (QSPR) for the transdermal delivery of NSAIDs. J. Controlled
632 Release. 138, 260-267.

633 MOE version 2011.10. Chemical Computing Group Inc. Montreal, Quebec, Canada,
634 http://www.chemcomp.com/, 2011.

635 Monene, L.M., Goosen, C., Breytenbach, J.C., Hadgraft, J., 2005. Percutaneous absorption of
636 cyclizine and its alkyl analogues. Eur. J. Pharm. Sci. 24, 239-244.

637 Moore, W.J., 1972. Physical Chemistry (5TH edition). Longman publishing, Prentice-Hall.

638 Nathan, D., Sakr, A., Lichtin, J.L., Bronaugh, R.L., 1990. *In vitro* skin absorption and
639 metabolism of benzoic-acid. p-aminobenzoic acid and benzocaine in the hairless guinea-pig.
640 Pharm. Res. 7, 1147-1151.

641 Nielsen, J.B., Nielsen, F., Sorensen J.A. 2004. *In vitro* percutaneous penetration of five pesticides
642 – Effects of molecular weight and solubility characteristics. Ann. Occup. Hyg. 48, 697-705.

643 OECD, Organisation For Economic Co-Operation And Development, OECD Guidance
644 Document No. 28: Guidance Document for the Conduct of Skin absorption studies. 2004a March
645 05. Available from:
646 http://www.oecd.org/officialdocuments/displaydocumentpdf?cote=env/jm/mono(2004)2&doclan
647 guage=en.

648 OECD, Organisation for Economic Co-operation and Development, OECD guideline for the
649 testing of chemicals. Test No. 428: Skin Absorption: In Vitro Method.; 2004b April 13. Available
650 from: http://www.oecdbookshop.org/oecd/display.asp?sf1=identifiers&st1=9789264071087.

651 Patil, S., Singh, P., Szolar-Platzer, C., Maibach, H.I., 1996. Epidermal enzymes as penetration
652 enhancers in transdermal drug delivery. J. Pharm. Sci. 85, 249-252.

653 Potts, R.O., Guy, R.H., 1992. Predicting skin permeability. Pharm. Res. 9, 663-669.

654 PubChem Home Page. accessed September 2010. Available from:
655 http://pubchem.ncbi.nlm.nih.gov/.

656 Riviere, J.E., Brooks, J.D., 2005. Predicting skin permeability from complex chemical mixtures.
657 Toxicol. Appl. Pharmacol. 208, 99-110.

658 Riviere, J.E., Brooks, J.D., 2011. Predicting skin permeability from complex chemical mixtures:
659 Dependency of quantuitative structure permeability relationshiops (QPSR) on biology of skin
660 model used. Toxicol. Sci. 119, 224-232.

661 Roberts, M.S., Cross, S.E., Pellett, M.A., 2002. Skin transport, in: Walters, K.A. (ds.),
662 Dermatological and transdermal formulations (Drugs and the Pharmaceutical Sciences Vol 119).
663 Marcel Dekker, New York, pp. 89-195.

664 Roberts, M.S., Walker, M., 1993. Water – the most natural penetration enhancer, in: Walters,
665 K.A., Hadgraft, J. (Eds.), Pharmaceutical Skin Penetration Enhancement. Marcel Dekker, New
666 York, pp. 1-30.

667 Rowe, R.C., Sheskey, P.J., Quinn, M.E., 2009. Handbook of pharmaceutical excipients (6th
668 edition). Pharmaceutical press.

669 Santos, P., Watkinson, A.C., Hadgraft, J., Lane, M.E., 2010. Oxybutynin permeation in skin: The
670 influence of drug and solvent activity. Int. J. Pharm. 384, 67-72.

671 Sartorelli, P., Andersen, H.R., Angerer, J., Corish, J., Drexler, H., Goen, T., Griffin, P.,
672 Hotchkiss, S.A.M., Larese, F., Montomoli, L., Perkins, J., Schmeiz, M., van de Sandt, J.,
673 Williams, F., 2000. Percutaneous penetration studies for risk assessment. Environ. Toxicol.
674 Pharmacol. 8, 133-152.

675 Scheuplein, R.J., Blank, I.H., Brauner, G.J., MacFarlane, D.J., 1969. Percutaneous Absorption of
676 Steroids. J. Invest. Dermatol. 52, 63-70.

677 Sigma-Aldrich. accessed Sep 2010. Available from: http://www.sigmaaldrich.com/sigma-
678 aldrich/.

679 Sinko, P.J., 2011. Martin's Physical Pharmacy and Pharmaceutical Sciences (6th edition).
680 Lippincott Williams & Wilkins publications.

681 Slovokhotov, Y.L., Batsanov, A.S., Howard, J.A.K., 2007. Molecular van der Waals symmetry
682 affecting bulk properties of condensed phases: melting and boiling points. Struct. Chem. 18, 477-
683 491.

684 SRC PhysProp database. Syracuse Research Corporation. accessed Nov 2010 – Feb 2011.
685 Available from: http://www.syrres.com/what-we-do/databaseforms.aspx?id=386.

686 Stott, W., Williams, A.C., Barry, B.W., 1997. Transdermal delivery from eutectic systems:
687 Enhanced permeation of a model drug. ibuprofen J. Controlled Release. 50, 297–308.

688 Surber, C., Wilhelm, K.P., Maibach, H.I., 1991. *In-vitro* skin pharmacokinetic of acitretin:
689 percutaneous absorption studies in intact and modified skin from three different species using
690 different receptor solutions. J. Pharm. Pharmacol. 43, 836-840.

691 Sznitowska, M., Janicki, S., Baczek, A., 2001. Studies on the effect of pH on the lipoid al route of
692 penetration across stratum corneum. J. Controlled Release. 76, 327-335.

693 Tang, H., Blankschtein, D., Langer, R., 2002. Prediction of steady-state skin permeabilities of
694 polar and nonpolar permeants across excised pig skin based on measurements of transient
695 diffusion: Characterization of hydration effects on the skin porous pathway. J. Pharm. Sci. 91,
696 1891-1907.

697 Van de Sandt, J.J.M., van Burgsteden, J.A., Carmichael, P.L., Dick, I., Kenyon, S., Korinth, G.,
698 Larese, F., Limasset, J.C., Maas, W.J.M., Montomoli, L., Nielsen, J.B., Payan, J.P., Robinson, E.,
699 Sartorelli, P., Schaller, K.H., Wilkinson, S.C., Williams, F.M., 2004. *In vitro* predictions of skin
700 absorption of caffeine. testosterone and benzoic acid: a multi-centre comparison study. Regul.
701 Toxicol. Pharmacol. 39, 271-281.

702 Watkinson, R.M., Herkenne, C., Guy, R.H., Hadgraft, J., Oliveira, G., Lane, M.E., 2009.
703 Influence of ethanol on the solubility, ionization and permeation characteristics of ibuprofen in
704 silicon and human skin. Skin Pharmacol. Physiol. 22, 15-21.

705 Wilkinson, S.C., Mass, W.J., Nielsen, J.B., Greaves, L.C., van de Sandt, J.J., Williams, F.M.,
706 2006. Interactions of skin of skin thickness and physicochemical properties of test compounds in
707 percutaneous penetration studies. Int. Arch. Occup. Environ. Health.79, 405-413.

708 Wilkinson, S.C., Mass, W.J.M., Nielsen, J.B, Greaves, L.C., van de Sandtt, J.J.M., Williams,
709 F.M., 2004. Influence of skin thickness on percutaneous penetration *in vitro,* in: Brain, K.R.,
710 Walters, K.A. (Eds.), Perspectives in percutaneous penetration, Vol 9a, Ninth international
711 Conference, La Grande Motte, France. STS Publishing, Cardiff, pp. 83

712 Wilkinson, S.C., Williams, F.M., 2002. Effects of experimental conditions on absorption of
713 glycol ethers through human skin *in vitro*. Int. Arch. Occup. Environ. Health. 75, 519-527.

714 Zhai, H., Maibach, H.I., 2001. Effects of skin occlusion on percutaneous absorption: an overview.
715 Skin Pharmacol. Appl. Skin Physiol. 14, 1-10.

716

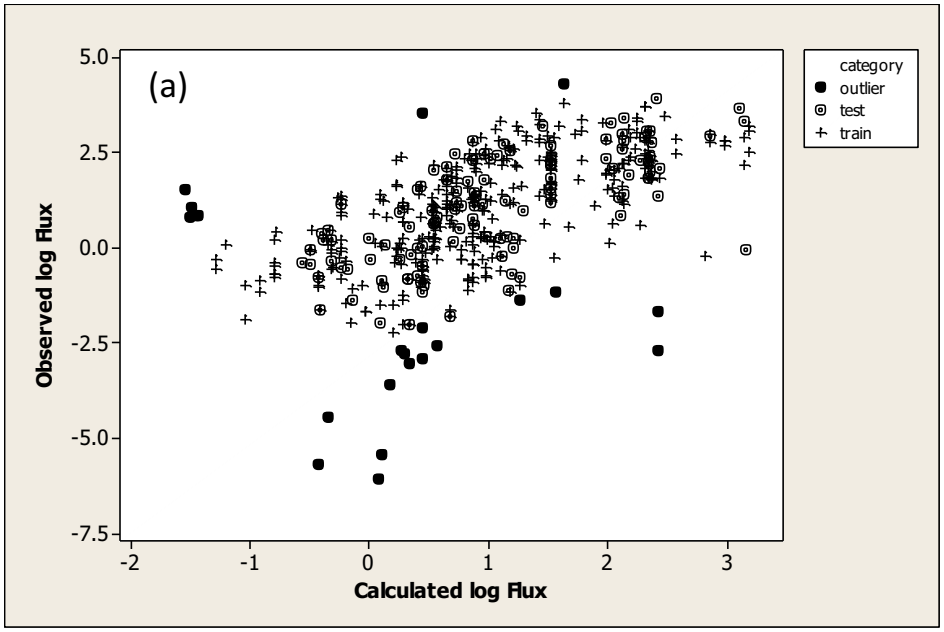

717

718

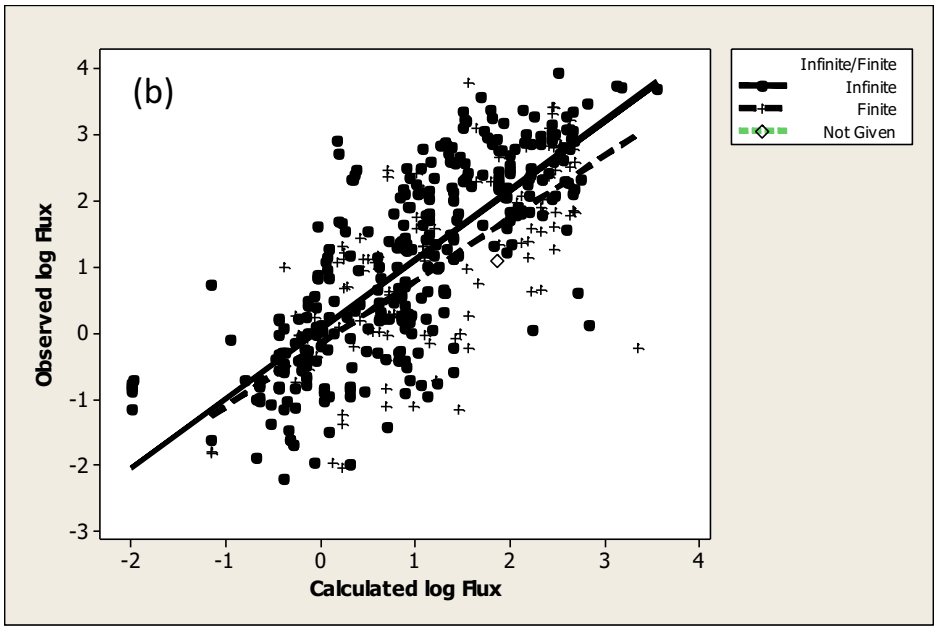

719

720

721

722

723

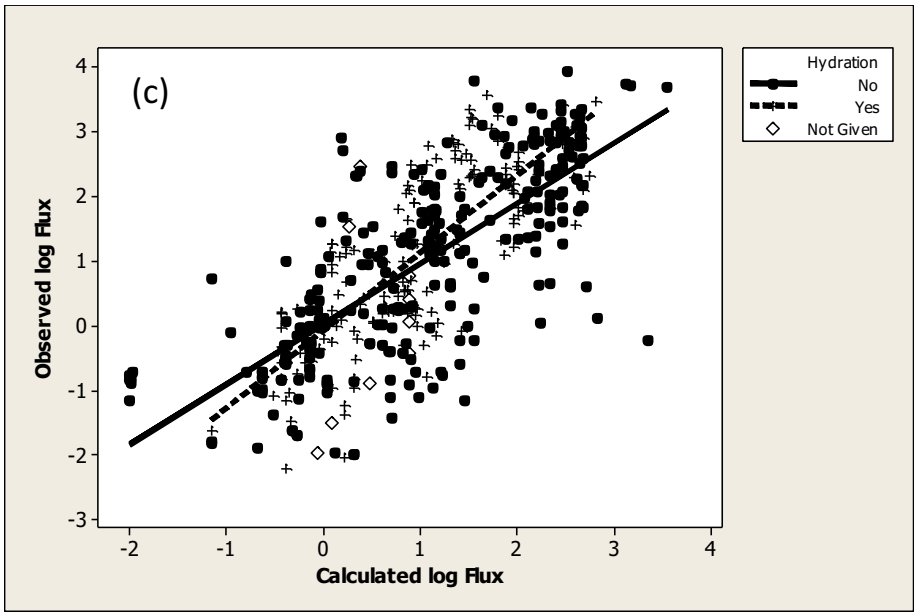

724

725 Figure 1. Observed log Flux against calculated log Flux by equation (3); Figure 1(a)
726 illustrates different groups: '+' indicates the training set, 'o' indicates the test set and '•'
727 indicates the outliers; Figure 1(b) shows the lines of best fit for the data obtained under
728 infinite (solid line) and finite (dashed line) dosing; Figure 1(c) shows the lines of best fit for
729 the data obtained from pre-hydrated (dashed line) or dry (solid line) skin.

730

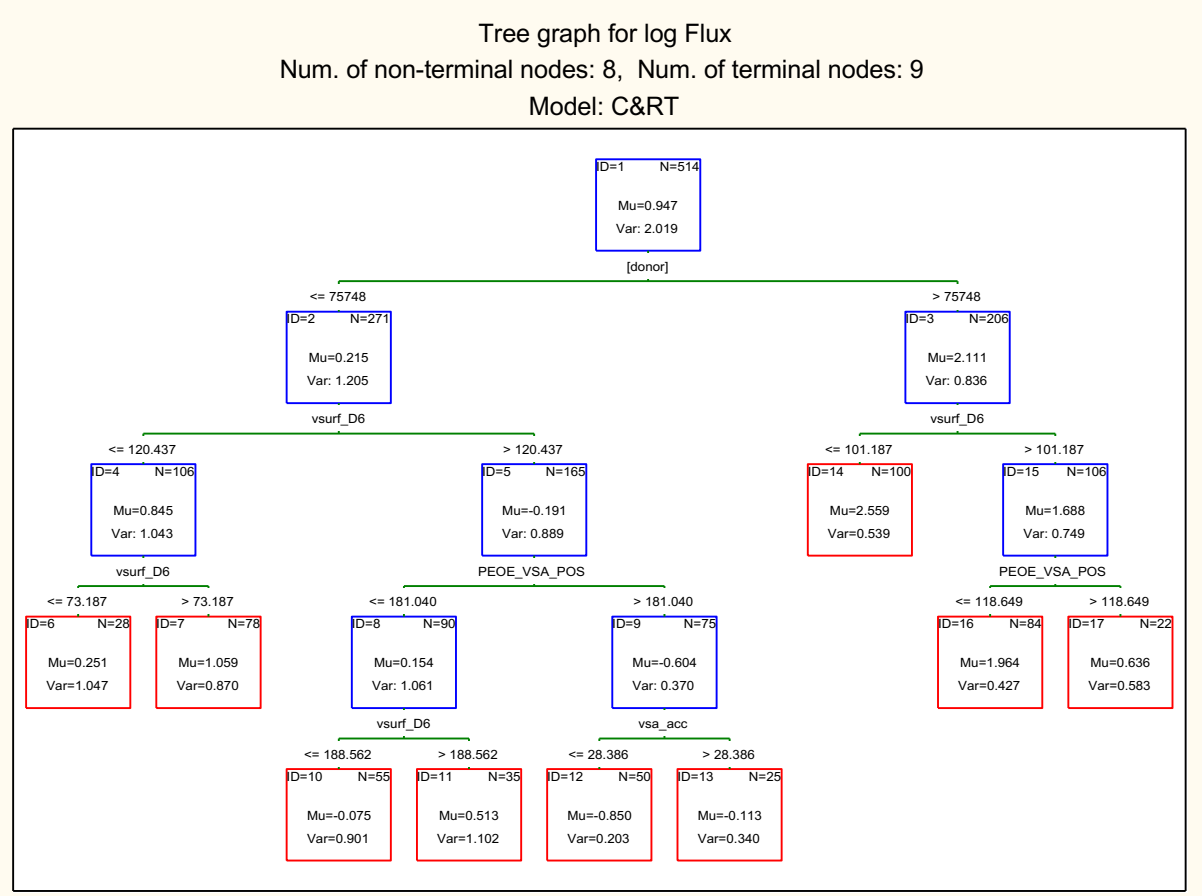

Figure 2. RT model (1), N is the number of data, Mu is the mean and Var is the variance of log Flux

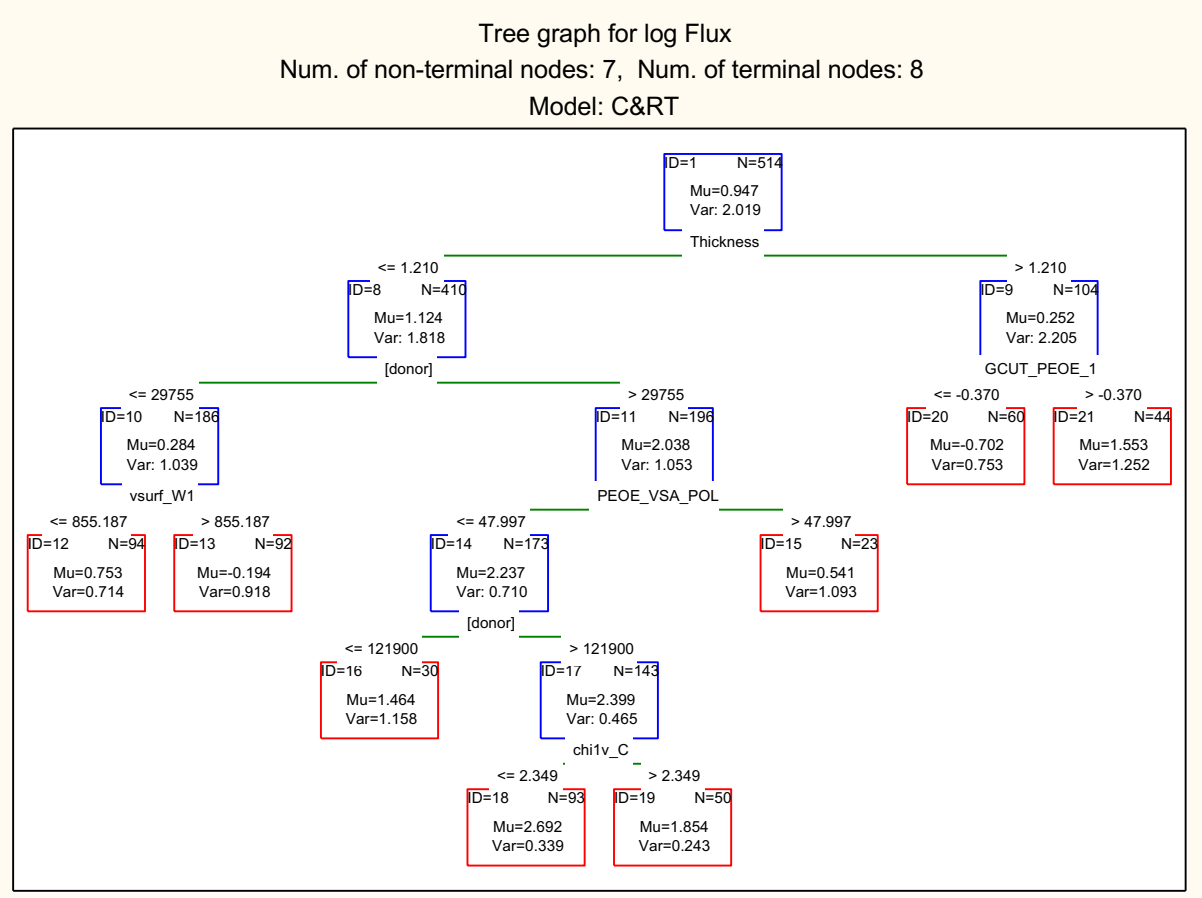

Figure 3. RT model (2) incorporating membrane thickness for the first partitioning, N is the number of data points, Mu is the average and Var is the variance of log Flux

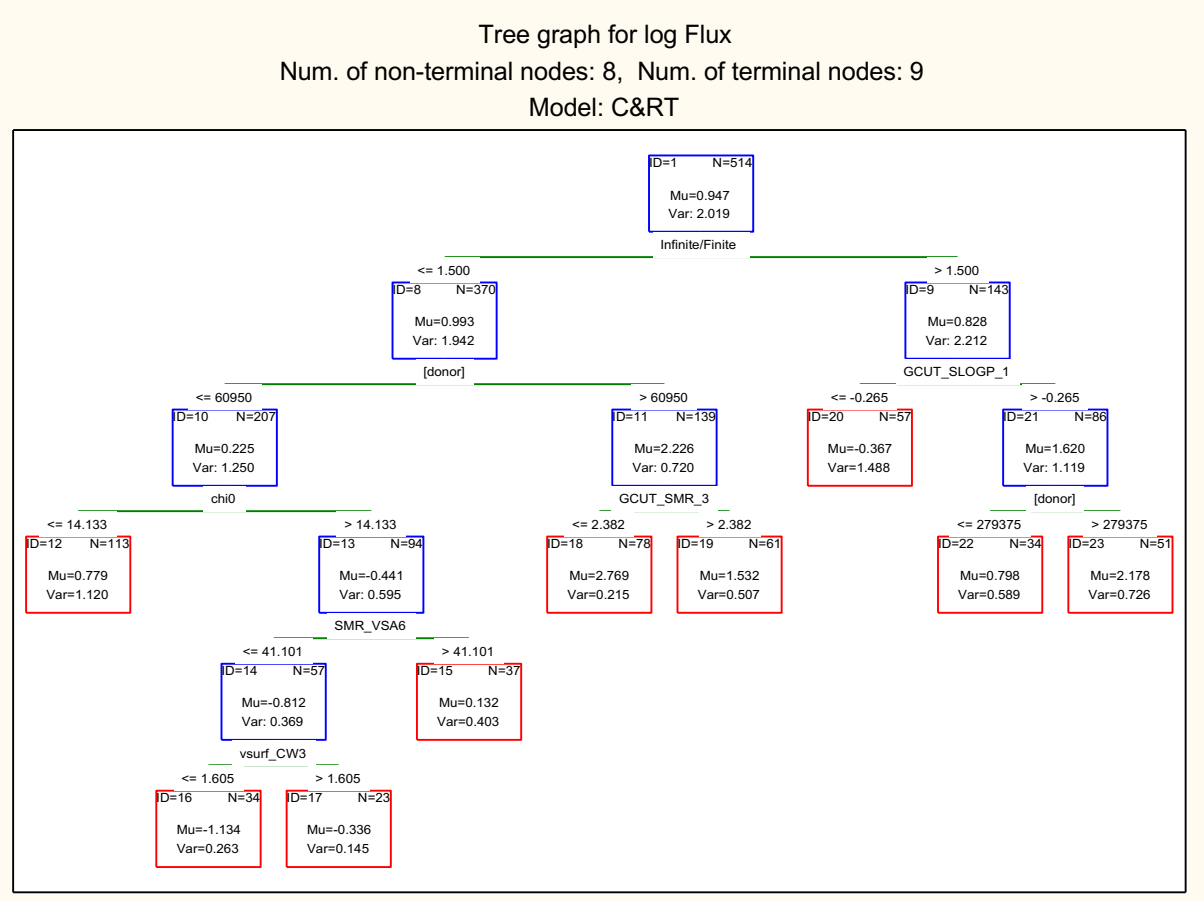

Figure 4. RT model (3) incorporating indicator variable for infinite or finite dose application, N is the number of data points, Mu is the average and Var is the variance of log Flux

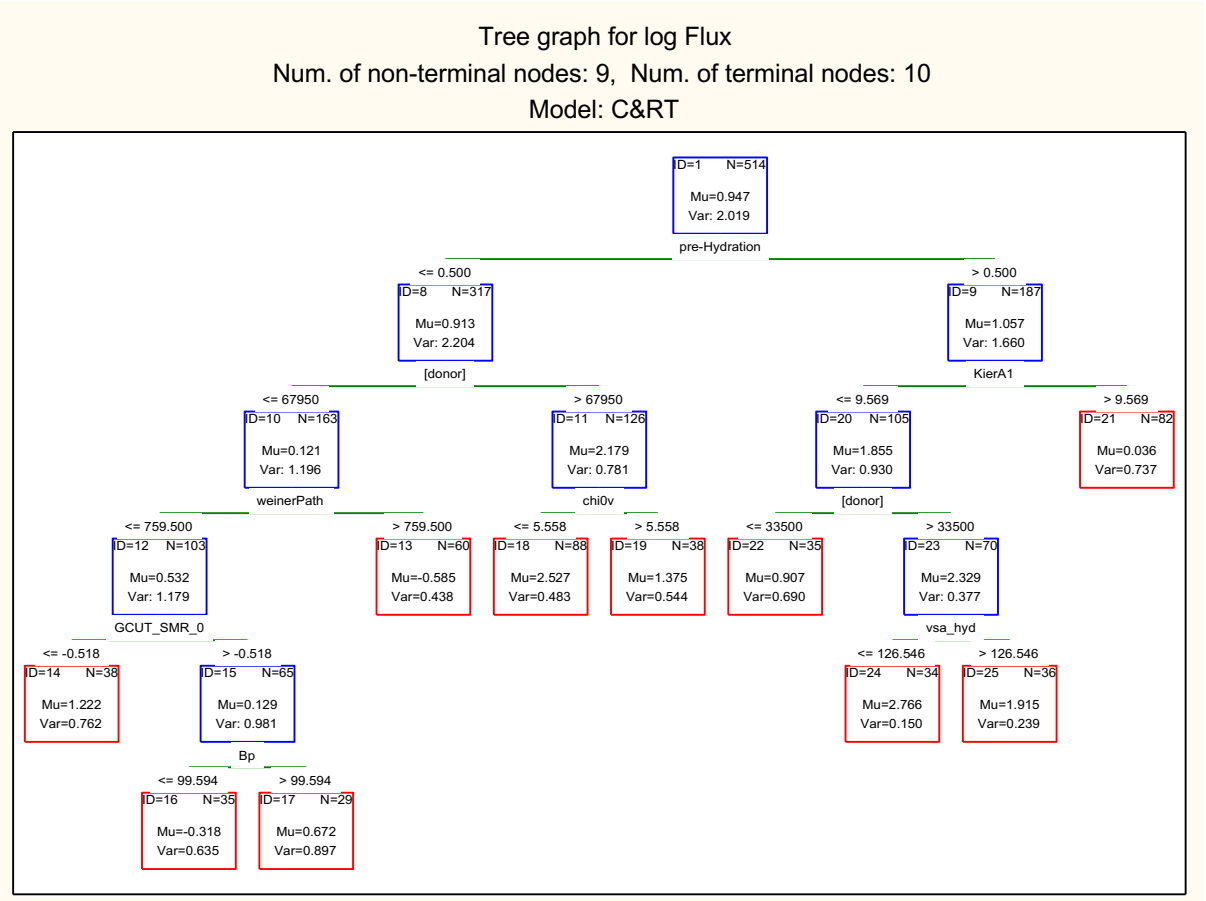

Figure 5. RT model (4) incorporating indicator variable for skin pre-hydration for the first partitioning, N is the number of data points, Mu is the average and Var is the variance of log Flux.

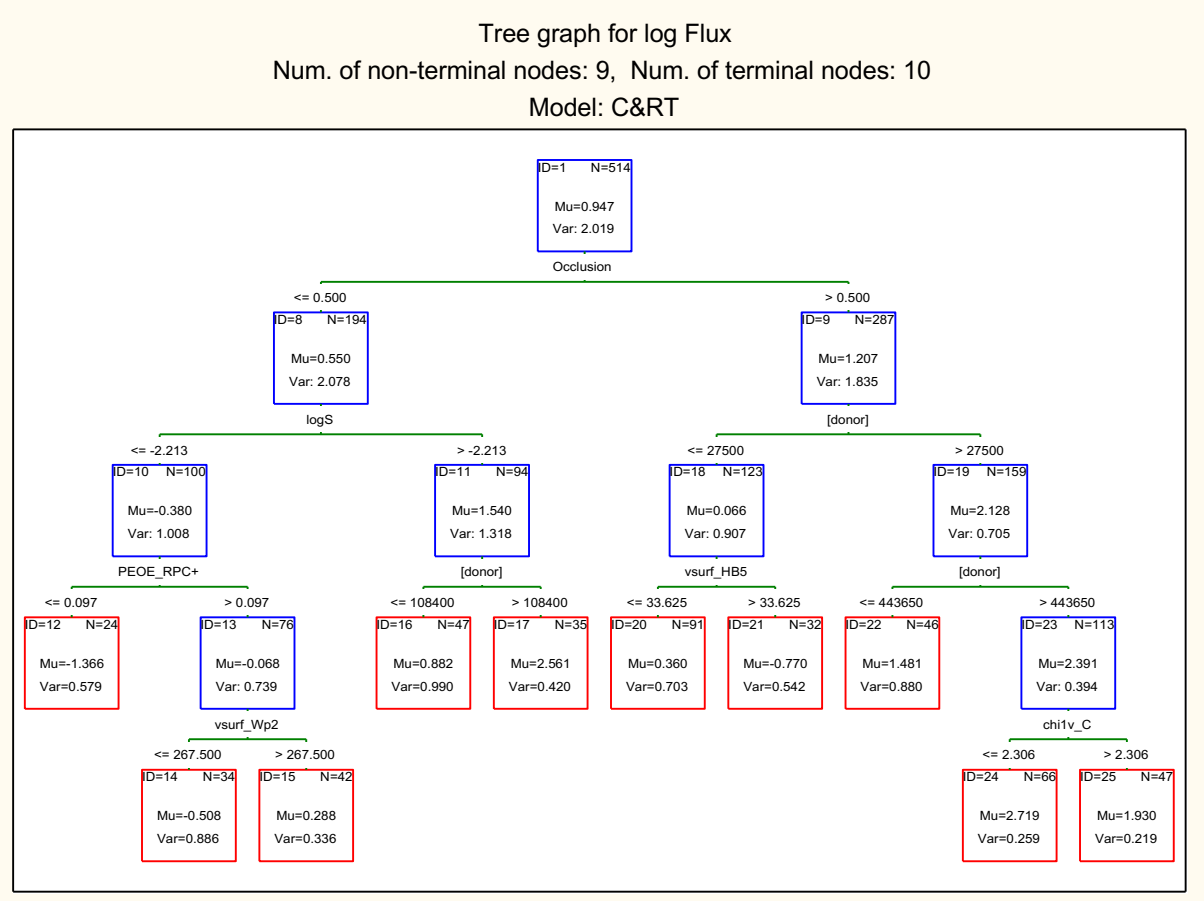

Figure 6. RT model (5) incorporating occlusion in the first partitioning, N is the number of data points, Mu is the average and Var is the variance of log Flux.

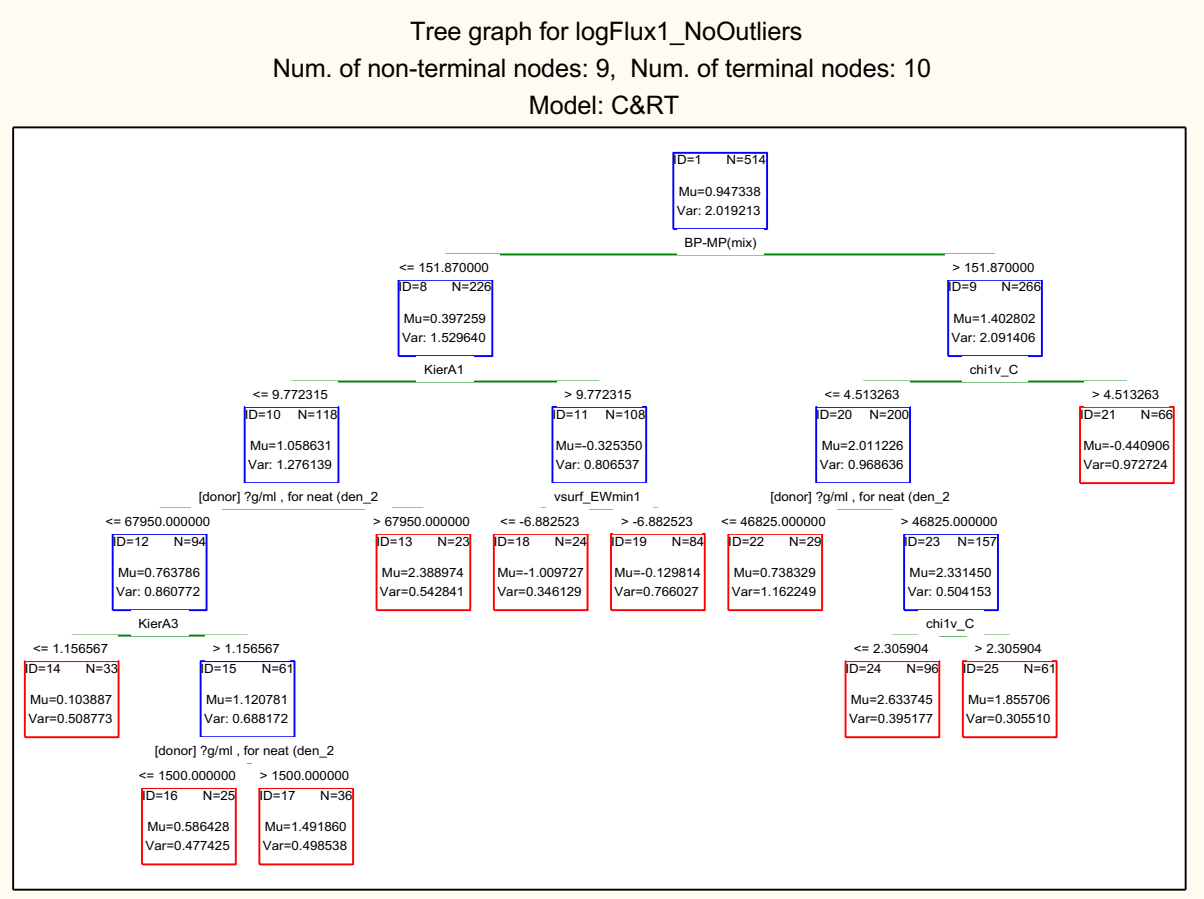

Figure 7. RT model (6) incorporating BP-MP(mix) as the first parameter for partitioning, N is the number of data points, Mu is the average and Var is the variance of log Flux.

Table 1. Statistical parameters of RT models

RT model	Experimental Parameter	MAE	Risk Estimate
(1)	-	0.625	0.643
(2)	Skin thickness	0.638	0.676
(3)	Exposure type	0.628	0.655
(4)	Pre-hydration	0.597	0.569
(5)	Occlusion	0.587	0.585
(6)	BP-MP(mix)	0.552	0.041

755

756